Observation of polarized luminescence from Jahn-Teller split states of self-trapped excitons in $PbWO_4$ by time-resolved spectroscopy

Minoru Itoh* and Tomonori Aoki

Department of Electrical and Electronic Engineering, Faculty of Engineering,

Shinshu University, 4-17-1 Wakasato, Nagano 380-8553, Japan

Abstract

Time-resolved luminescence spectra of oriented $PbWO_4$ crystals have been measured for the polarizations with the electric vector parallel to the crystallographic *c* axis (**E**//**c**) and perpendicular to it (**E**⊥**c**). All the three emission bands (I, II and III) due to the Jahn-Teller spit states of a self-trapped exciton (STE) located on $(WO_4)^{2-}$ complex anion are found to exhibit significant polarizations in the *ac* plane. The main band II peaking at 425 nm is polarized with **E**//**c** at low temperatures ($T < 100$ K), but changes its polarization from **E**//**c** to **E**⊥**c** at $T > 150$ K. The band III at 450 nm is polarized with **E**⊥**c** at $T = 230$ and 300 K. The degree of polarization of these two bands does not depend on the polarization of excitation light. On the other hand, the band I at 407 nm is polarized with **E**⊥**c** (**E**//**c**) under the photoexcitation polarized parallel (perpendicular) to the *c* axis, in the temperature range of $T = 150–300$ K. The observed polarization characteristics of three emission bands invoke further lowering of symmetry of tetrahedral $(WO_4)^{2-}$ ions due to the uniaxially compressive crystal field, in addition to the Jahn-Teller distortion. The sublevels of the STEs responsible for the $PbWO_4$ luminescence are assigned on the basis of a group-theoretical consideration.

PACS: 71.35. –y, 71.70. –d, 78.55.Hx

Keywords: photoluminescence, polarization, time-resolved spectroscopy, Jahn-Teller effect,

adiabatic potential energy surface, self-trapped exciton, $PbWO_4$

---

* Corresponding author; E-mail address: itohlab@shinshu-u.ac.jp, Phone: +81-26-269-5261, Fax: +81-26-269-5220

1. Introduction

The tungstate and molybdate families are classified into two groups from the point of view of crystal structure; one is the scheelite structure based on independent WO_4 (MoO_4) tetrahedra separated by counterions and the other is the wolframite structure based on WO_6 (MoO_6) octahedra with shared oxygen ions [1, 2]. Lead tungstate $PbWO_4$ (PWO) is representative of scheelite-type tungstates with the space group $I4_1/a$. The PWO crystal is tetragonal and therefore optically uniaxial. The optical axis is parallel to the crystallographic *c* axis, while the *a* and *b* axes are equivalent to each other. In PWO crystal, a Pb ion is eightfold coordinated by oxygen ions, and each W ion is surrounded by four equivalent O ions to form $(WO_4)^{2-}$ oxyanion molecule. There are four crystallographically equivalent $(WO_4)^{2-}$ tetrahedra per unit cell.

The intrinsic luminescence of PWO is totally structureless, having a peak at around 425 nm, and has drawn much attention as a promising candidate for scintillation detectors in high-energy particle physics [3, 4] and in positron emission tomography (PET) for medical diagnosis of cancers and other diseases [5, 6]. This blue luminescence is ascribed to the radiative recombination of a self-trapped exciton (STE) located on $(WO_4)^{2-}$ molecular ion [7, 8]. In a free $(WO_4)^{2-}$ ion with tetrahedral symmetry T_d, two singlet and two triplet states are expected to result from the $(t_1)^5(e)^1$ excited configuration: $^1T_2 > {}^1T_1 > {}^3T_2 \cong {}^3T_1$. It has long been accepted [9] that the intrinsic PWO luminescence originates from the $^3T_1$ and (or) $^3T_2 \rightarrow {}^1A_1$ transition, which is spin-forbidden but is partially allowed by the spin-orbit interaction with the upper-lying singlet $^1T_{1,2}$ states.

Recently, the above model has been shown to be so simple that it cannot explain the composite nature of the PWO luminescence revealed by our time-resolved experiments [10, 11]. The time-resolved luminescence of PWO is composed of four emission bands peaking at 407 nm (I), 425 nm (II), 450 nm (III) and 490 nm (IV); the first three bands are intrinsic to PWO, and the last one coincides with the green luminescence originating from lattice imperfections. Appearance of the three intrinsic bands I, II and III is nicely explained by taking a Jahn-Teller (JT) effect into account. The symmetry lowering of $(WO_4)^{2-}$ ions from T_d to C_{3v} due to the JT effect lifts the degeneracy of the $^3T_1$ and $^3T_2$ states. The former splits

into the $^3A_2$ and ^3E sublevels, and the latter into the $^3A_1$ and ^3E sublevels. The situation is schematically illustrated in Fig. 1, where the energy separation between $^3T_1$ and $^3T_2$ is assumed to be very small. It is to be noted that a group-theoretical approach does not say anything about the order of each sublevel on an energy scale.

A well-known example of the JT effect is the emission from Tl^+-type impurity centers, with O_h symmetry in the ground state, in alkali halides, where the tetragonal JT distortion removes the degeneracy of the relaxed excited states and results in two minima of the adiabatic potential energy surfaces (APESs) in a configuration coordinate diagram [12, 13]. Two kinds of emission bands are therefore observed. A theoretical analysis of the JT effect has been made for more complex species like $(WO_4)^{2-}$ molecular ions by Bacci *et al*. [14, 15]. They have proposed that, owing to the trigonal JT distortion, the lowest triplet states of PWO split into three APESs, the middle of which emits the most intense luminescence. Their proposal is fairly consistent with our observation of three intrinsic emission bands in PWO [10, 11]. The importance of the JT effect for the triplet luminescence in tungstates and molybdates has also been pointed out from a series of optically detected magnetic resonance experiments by van der Waals's group [16-18].

The polarization of luminescence in PWO has been investigated by several groups [7, 19-22]. There is no consistency between their results, however. The authors of [7, 19 and 20] revealed that the blue (intrinsic) luminescence is unpolarized, whereas the green (extrinsic) luminescence is primarily polarized at T = 77 and 300 K. On the other hand, Reut [21, 22] performed systematic studies on the polarization of the intrinsic luminescence in a number of scheelite-structured tungstates and molybdates in the range T = 77–400 K. He found that the intrinsic PWO luminescence is clearly polarized, with the temperature-dependent degree of polarization. All these previous experiments have been carried out by observing the total (i.e., time-integrated) luminescence under steady-state excitation by polarized light. Because of the composite nature of the PWO luminescence clarified recently, this may be one of possible reasons for the discrepancies mentioned above, suggesting an essential need to make the combined measurements of polarization and time-resolved luminescence spectra.

In the present study, we have investigated the polarization of time-resolved luminescence

spectra of oriented PWO crystals excited by linearly polarized light. Since the tetragonal PWO is a birefringent crystal, only light linearly polarized either parallel or perpendicular to the crystallographic *c* axis will preserve its polarization state on passing through the crystal. This property restricts the determination of the polarization of luminescence to the components polarized parallel or perpendicular to the *c* axis. The measurements are performed in a wide temperature range of T = 8–300 K. The results clearly reveal that the intrinsic bands I, II and III, as well as the extrinsic band IV, are significantly polarized in the *ac* plane. Based on the observed polarization characteristic of each intrinsic emission band, the sublevels of the luminescent triplet STE states in PWO are discussed and assigned with the help of a group-theoretical consideration. The luminescent state responsible for the defect-related band IV is also discussed in brief.

2. Experiment

Single crystals of PWO used in the present experiment were grown by the Czochralski method with a platinum crucible using the starting raw materials of PbO and WO_3 (nominally 5 N purity) in the three-time crystallization. A chemical analysis showed that any unwanted impurities are at a level below 5 ppm. The samples were polished to optical grade over all surfaces, having a size of $7 \times 6 \times 2$ mm^3. The orientation of the crystal axes was determined by means of x-ray diffraction. A sample with the *ac* surface plane was mounted with its *c* axis vertical on the copper holder which allowed for optical access in the horizontal plane. The sample holder was placed in a closed-cycle He optical cryostat working in the temperature range between 8 and 300 K.

The fourth harmonics (266 nm) of a *Q*-switched neodymium-doped yttrium aluminum garnet (Nd:YAG) laser (Continuum Minilite II) was used as an excitation light source. The 266 nm light locates in the high-energy region of the exciton absorption band of PWO [23, 24]. The pulse width, repetition rate and power density on the sample surface were 7 ns, 10 Hz and 10 MW/cm^2, respectively. An electronic synchronization technique was applied by using a digital delay-pulse generator (BNC Model 555). The time jitter of the system was ±20 ns. The polarization of laser light was varied in either direction parallel or perpendicular

to the *c* axis by using a half-wave plate. The incident angle of laser light was nearly normal to the sample surface, and luminescence signals from the irradiated surface were observed along the 30° direction relative to the laser beam. After passing through a linear polarizer, the luminescence was focused by a convex lens onto the entrance slit of a Jobin-Yvon HR320 monochromator equipped with a gated intensified charge-coupled device camera (Hamamatsu C5909-06), with a spectral resolution of 10 nm. A quartz depolarizer was installed just in front of the entrance slit of the monochromator, in order to eliminate any influence of the polarization characteristics of the analyzing system (mainly caused by the monochromator grating). The luminescence spectra were not corrected for the spectral response of the detection system; in fact, it was not so dependent on the wavelength in the region of interest. Such a correction is needed if time-resolved luminescence spectra are decomposed into some individual bands by using a Gaussian shape, but not essential in our analysis where spectrum decompositions are performed thanks to experimentally determined band shapes.

3. Results

Time-resolved luminescence spectra were measured for polarizations **E**//**c** and **E**⊥**c** under the excitation by light polarized parallel to the *c* axis (**E**$_{ex}$//**c**) or perpendicular to it (**E**$_{ex}$⊥**c**). The delay time τ_D was changed from 0 to 1 ms, with a gate width Δt ranging from 50 ns to 1 ms. In what follows we shall define the degree of polarization as

$$P = \frac{I(\mathbf{E}//\mathbf{c}) - I(\mathbf{E}\perp\mathbf{c})}{I(\mathbf{E}//\mathbf{c}) + I(\mathbf{E}\perp\mathbf{c})}, \quad (1)$$

where I(**E**//**c**) and I(**E**⊥**c**) are the intensities of luminescence polarized with **E**//**c** and **E**⊥**c**, respectively.

Typical results obtained under the photoexcitation with **E**$_{ex}$//**c** and **E**$_{ex}$⊥**c** at T = 75 K are presented in Figs. 2(a) and 2(b), respectively. Blue solid and broken lines show the spectra for **E**//**c** and **E**⊥**c**, respectively. The spectra in (a) and (b) are normalized to unity at their maxima measured for **E**//**c**. From Fig. 2, one may recognize the following three points. (i) No significant changes in spectral shape and peak position are seen in the range of τ_D = 0–1

ms. Only the main band II, having a peak at 425 nm, is observed. Since the band II is very intense and has a long decay time (≈ 6 μs) at low temperatures (T < 150 K) [25], the other three bands I, III and IV are completely masked by band II at 75 K. (ii) The value of P does not change even if τ_D is varied, and is nearly +0.17. (iii) The value of P is almost the same in both polarizations $\mathbf{E}_{ex}//\mathbf{c}$ and $\mathbf{E}_{ex}\perp\mathbf{c}$ of excitation light.

Time-resolved luminescence spectra for $\mathbf{E}//\mathbf{c}$ and $\mathbf{E}\perp\mathbf{c}$ observed under the photoexcitation with $\mathbf{E}_{ex}//\mathbf{c}$ at T = 300 K are shown in Figs. 3(a) and 3(b), respectively. The spectra measured at the same delay time are normalized to unity at their maxima. Therefore, one can compare the relative intensities of (a) and (b) at their respective delay times.

The time-resolved spectra in Fig. 3 exhibit a composite nature; for example, the peak position at τ_D = 500 ns is slightly red-shifted by 10 nm relative to that at τ_D = 0, and further red-shift is seen at τ_D = 2 μs. Fortunately, spectral shapes of three emission bands I, II and IV can be obtained from our experimental results. By making use of these well-determined band shapes, the time-resolved spectra in Fig. 3 are decomposed into four individual bands with different decay times. The details of the decomposition procedure are found in [11]. An isolated band appears at 407 nm in the range of τ_D = 5–400 μs, which is labeled I (indicated by violet dotted line). A band is observed at around 425 nm just after the pulse excitation (τ_D = 0) and is labeled II (blue solid line). A band peaking at 490 nm is seen when τ_D is as long as 1 ms, which is labeled IV (green solid line). The experimentally obtained spectra are not reproduced by only these three emission bands, especially in the range of τ_D = 500 ns–2 μs. A band centered at around 450 nm is required to achieve a good agreement with the experimental data. This band is labeled III (light-blue broken line). The sum of the four individual bands is presented by a red solid line.

From a comparison of Fig. 3(a) and Fig. 3(b), it is obvious that the intensities of four bands in (b) are stronger than those in (a): P (I) = –(0.28 ± 0.02), P (II) = –(0.20 ± 0.02), P (III) = –(0.12 ± 0.04) and P (IV) = –(0.14 ± 0.02). The errors of P are estimated from the uncertainty of the emission intensities due to the spectrum decomposition into the four bands.

Time-resolved luminescence spectra for $\mathbf{E}//\mathbf{c}$ and $\mathbf{E}\perp\mathbf{c}$ observed under the photoexcitation

with $\mathbf{E}_{ex}\perp\mathbf{c}$ at T = 300 K are shown in Figs. 4(a) and 4(b), respectively. The color and line indications of the respective bands are the same as Fig. 3. Since the emission intensity under the $\mathbf{E}_{ex}\perp\mathbf{c}$ excitation was weak compared to that under the $\mathbf{E}_{ex}//\mathbf{c}$ excitation, the spectra of Fig. 4 are relatively noisier than those of Fig. 3. Comparing Fig. 4(a) with Fig. 4(b), we obtain P (I) = +(0.26 ± 0.02), P (II) = –(0.19 ± 0.02), P (III) = –(0.11 ± 0.04) and P (IV) = –(0.15 ± 0.02). The values of P do not depend on the polarization of excitation light, except for band I. This band is polarized in the $\mathbf{E}\perp\mathbf{c}$ direction under the $\mathbf{E}_{ex}//\mathbf{c}$ excitation and polarized in the $\mathbf{E}//\mathbf{c}$ direction under the $\mathbf{E}_{ex}\perp\mathbf{c}$ excitation. Another striking result recognized from Figs. 2–4 is the polarization change of band II from $P > 0$ to $P < 0$ when T is varied from 75 to 300 K.

The temperature dependence of P was investigated for all the four bands under both polarizations of excitation light. The result of band II is shown in Fig. 5, where black open circles correspond to the results of $\mathbf{E}_{ex}//\mathbf{c}$ and red closed circles to those of $\mathbf{E}_{ex}\perp\mathbf{c}$. The II band is primarily polarized with $\mathbf{E}//\mathbf{c}$ at $T < 80$ K, having $P \approx +0.17$. When T is raised, the value of P begins to decrease at 100 K, changes its sign from positive to negative at around 150 K, and eventually reaches –(0.20 ± 0.02) at 300 K, irrespective of the polarization of excitation light. In Fig. 5, the solid line is the best-fitted curve of Eq. (4) described later.

As noted before, the bands I, III and IV are observable in the temperature range of $T > 150$ K, in which the decay time of band II becomes comparable to or faster than those of these bands. The temperature dependences of P of bands I, III and IV in the 150–300 K range are shown by circles, triangles and squares in Fig. 6, respectively, where open symbols refer to the results of $\mathbf{E}_{ex}//\mathbf{c}$ and closed symbols to those of $\mathbf{E}_{ex}\perp\mathbf{c}$. The solid lines are depicted for guide to the eye. It appears that the values of P are fairly constant for bands I and III, while that for band IV is appreciably temperature-dependent.

4. Discussion

The present experiment indicates that the intrinsic bands I, II and III, as well as the extrinsic band IV, in PWO are significantly polarized in either direction parallel or perpendicular to the crystal c axis. This result is partly consistent and partly inconsistent with

the earlier results by Groenink and Blasse [7], van Loo [19] and Korzhik *et al*. [20]. They have reported that the blue luminescence exhibits no appreciable polarization, while the green luminescence is strongly polarized, although the polarization direction referred to the crystallographic axes is not clearly described in their papers. The latter result is consistent with the present result, but the former result is inconsistent with it. Reut [22] has reported that the blue luminescence is polarized with **E**//**c** at $T < 100$ K, and changes its polarization from **E**//**c** to **E**⊥**c** at $T > 150$ K. His finding is in good agreement with our result, taking into account the fact that the band II has a dominant contribution to the time-integrated luminescence in PWO. The failure of the other researchers [7, 19 and 20] to observe the polarized blue luminescence may be accounted for by assuming that the samples used by them contain a considerable amount of lattice defects emitting the green luminescence polarized with **E**⊥**c** (see also the last paragraph of this section). If this assumption is correct, negatively polarized green luminescence could compensate the positive polarization of band II at low temperatures (e.g., $T = 77$ K), thus leading to no or little polarization of the "blue" luminescence. When T is increased up to 300 K, the band II is thermally quenched [11]. As a result, the polarized green luminescence becomes a substantial component, which is to be expected from the observations in [7, 19 and 20].

Let us first consider the polarization characteristics of the three intrinsic bands I, II and III. The polarization characteristic of the extrinsic band IV will be briefly discussed later. As is well known [7, 8], an exciton in tungstates is self-trapped on a $(WO_4)^{2-}$ molecular ion. Figure 7(a) illustrates a tetrahedral $(WO_4)^{2-}$ complex anion with respect to the crystal *c* axis, in which one tungsten (W) and four oxygen (O_1, O_2, O_3 and O_4) ions are presented as open and gray circles, respectively. The direction of the oxygen bridge O_1–O_2 (O_3–O_4) in a $(WO_4)^{2-}$ ion in tungstates, lying in the *ab* plane, is rotated away by 28–32° from the *a* (*b*) axis [26]. The intrinsic luminescence of PWO originates from the lowest triplet states of the STEs. The lowest triplet $^3T_2$ and $^3T_1$ states split into four sublevels $^3A_1$, ^3E, $^3A_2$ and ^3E, owing to the JT distortion of $(WO_4)^{2-}$, as shown in Fig. 1. The ground singlet state is of A_1 symmetry. The tetrahedron tends to a trigonal pyramid upon excitation. A JT-distorted $(WO_4)^{2-}$ ion with C_{3v} symmetry is schematically illustrated in Fig. 7(b). The *z* axis lies

exactly along the W–O_1 bond and coincides with the triad axis that carries the lattice into itself by a rotation of $2\pi/3$ radian. The *x* and *y* axes are defined as being perpendicular to the *z* axis.

In C_{3v} symmetry, the electric dipole transition $^3A_1 \rightarrow {}^1A_1$ is allowed for the polarization **E**//**z**, and the electric dipole transition $^3E \rightarrow {}^1A_1$ is allowed for the polarizations **E**//**x** and **E**//**y**. The optical transition $^3A_2 \rightarrow {}^1A_1$ is dipole forbidden. Here we have to notice two important points for JT-distorted $(WO_4)^{2-}$ ions in PWO: (1) The *z* axis does not coincide with the crystal *c* axis. (2) For the triad axis along W–O_1 bond, the corresponding axes along W–O_2, W–O_3 and W–O_4 bonds are found by rotation of 180°, 270° and 90° around the *c* axis, respectively. In other words, there are four equivalent triad axes along the W–O_1, W–O_2, W–O_3 and W–O_4 bonds. Therefore, the emission intensity I(**E**//**c**) is equal to I(**E**⊥**c**), even if the optical transition $^3A_1 \rightarrow {}^1A_1$ is polarized with **E**//**z**; i.e., it is impossible to detect any difference between I(**E**//**c**) and I(**E**⊥**c**). The same equality also holds for the transition $^3E \rightarrow {}^1A_1$ with the polarization **E**//**x** or **E**//**y**. It is thus concluded that no polarization is observed for the intrinsic PWO luminescence as far as the $(WO_4)^{2-}$ tetrahedron retains the C_{3v} symmetry, which is in clear contrast with our findings.

According to the neutron diffraction data [26], the $(WO_4)^{2-}$ tetrahedra in scheelite crystals are in reality distorted by compression along the *c* axis. This uniaxial crystal field lowers the symmetry of $(WO_4)^{2-}$ species in the ground state from T_d to D_{2d}. The combination of the JT coupling and the uniaxial crystal field would thus reduce the symmetry of $(WO_4)^{2-}$ upon excitation from C_{3v} to C_s. In Fig. 8 are presented the orientations of the fine structure axis ("spin axis") for one of the excited $(WO_4)^{2-}$ species with respect to the crystallographic axes and also relative to the four oxygen ions in the ground state [16]. The mirror plane σ_d spanned by O_1–W–O_2 in Fig. 8 is the only symmetry element in C_s symmetry. The *y* fine-structure axis is almost perpendicular to the σ_d plane. The *z* fine-structure axis is close to being parallel to the W–O_1 bond and lies together with the *x* fine-structure axis approximately in the σ_d plane. The orientations *x*, *y* and *z* of the transition dipole moments coincide, to a good approximation, with those of the corresponding fine-structure axes [16], both being not distinguished in this paper.

In C_s symmetry, the four excited levels, A_1, E, A_2 and E, derived in C_{3v} symmetry are transformed as follows; $A_1 \rightarrow A'(\mathbf{x})$ or $A'(\mathbf{z})$, $E \rightarrow A''(\mathbf{y})$ and $A'(\mathbf{x})$ or $A'(\mathbf{z})$, and $A_2 \rightarrow A''(\mathbf{y})$. Here, the vectors **x**, **y** and **z** in parentheses correspond to the orientations *x*, *y* and *z* of the transition dipole moments, respectively. The transitions from all the excited states of A'-type and A''-type to the ground state of A'-type are optically allowed. A complication arises because the dipole-moment axes *x*, *y* and *z* do not coincide with the crystal axes *a*, *b* and *c*. The intensities of the **x**-, **y**- and **z**-polarized light are proportional to the square of the direction cosine θ of the respective angles with the crystal axes **a**, **b** and **c**. The values of $\cos\theta$ in scheelite $PbMoO_4$, which has the same crystal structure as PWO, have been determined from the EPR experiments by van Tol and van der Waals [18]. We assume that the same values are applicable to PWO. The **x**-polarized light has $\cos\theta = 0.29$, 0.01 and 0.96 with respect to **a**, **b** and **c**, respectively. The **y**-polarized light has $\cos\theta = -0.53$ (**a**), 0.84 (**b**) and 0.10 (**c**). The **z**-polarized light has $\cos\theta = -0.82$ (**a**), –0.51 (**b**) and 0.28 (**c**). From these results, it is reasonable to suppose that the **x**-polarized light is a predominant component of $I(\mathbf{E}//\mathbf{c})$, with a small contribution to $I(\mathbf{E}\perp\mathbf{c})$, whereas the **y**- or **z**-polarized light largely contributes to $I(\mathbf{E}\perp\mathbf{c})$, with a small amount of $I(\mathbf{E}//\mathbf{c})$. That is to say, one can expect $P > 0$ for **x** and $P < 0$ for **y** and **z**.

Following the arguments above, we consider the excited states responsible for the main band II. At low temperatures, band II is primarily polarized with the electric vector along the *c* axis, $P = 0.17$ at 75 K. On raising the temperature, relative contribution of the emission component polarized perpendicular to the *c* axis increases and eventually becomes larger than the **E**//**c** polarized component, $P = -0.20$ at 300 K. This observation could be attributed to the thermal population of a very intensely radiative level lying above the metastable level and having an opposite polarization. Such a two-level model is illustrated by the inset of Fig. 5, in which the upper level is labeled as 2, and the lower (metastable) level as 1. The separation energy between the two levels is expressed by Δ. In such a two-level model, the intensities of the emission components polarized in the **E**//**c** and **E**$\perp$**c** directions are given as

$$I(\mathbf{E}//\mathbf{c}) = A_{//1} + A_{//2} \exp(-\Delta/k_B T), \qquad (2)$$

and

$$I(\mathbf{E}\perp\mathbf{c}) = A_{\perp 1} + A_{\perp 2}\exp(-\Delta/k_{\mathrm{B}}T), \tag{3}$$

respectively, where $A_{//1}$ and $A_{\perp 1}$ are the radiative transition probabilities from level 1 in the direction parallel and perpendicular to the *c* axis, respectively, and $A_{//2}$ and $A_{\perp 2}$ are the corresponding ones from level 2, and k_{B} is the Boltzmann constant. By substituting Eqs. (2) and (3) to Eq. (1), one obtains

$$P = \frac{(A_{//1} - A_{\perp 1}) + (A_{//2} - A_{\perp 2})\exp(-\Delta / k_{\mathrm{B}}T)}{(A_{//1} + A_{\perp 1}) + (A_{//2} + A_{\perp 2})\exp(-\Delta / k_{\mathrm{B}}T)}. \tag{4}$$

The total transition probability ($A_{//1} + A_{\perp 1}$) from level 1 is not clear from the present experiment, and therefore, it is normalized to unity. The solid line in Fig. 5 is the best-fitted curve of Eq. (4) to the experimental points. From the fit, we obtain ($A_{//1} - A_{\perp 1}$) = 0.17, ($A_{//2} + A_{\perp 2}$) = 220, ($A_{//2} - A_{\perp 2}$) = –44 and Δ = 72 ± 5 meV. The present value of Δ agrees well with the result (68 meV) by Reut [22]. As mentioned above, the total transition probability ($A_{//2} + A_{\perp 2}$) from level 2 is indeed much larger than that from level 1. The level 1 has a polarization characteristic $P > 0$ since $A_{//1} > A_{\perp 1}$, whereas the level 2 is characterized by $P < 0$ since $A_{\perp 2} > A_{//2}$.

As was found in [11], the emission intensity of band II decreases at high temperatures ($T >$ 150 K). This decrease is caused by the thermal quenching or disintegration of STEs, with an activation barrier $\Delta E \approx 230$ meV [27, 28]. It should be noted that the polarization change of band II begins at $T \approx 100$ K with Δ = 72 meV, which is more than three times smaller than ΔE. Therefore, it might be supposed that the temperature dependence of *P* for band II is hardly influenced by the thermal quenching phenomenon.

There is an interesting finding on the main band II. Nikl *et al*. [29] have revealed that the blue luminescence of PWO shows an order of magnitude increase of the decay time at very low temperatures ($T < 5$ K). This fact indicates the presence of a pair of closely spaced energy levels, the origin of which has not been discussed in [29]. The energy distance δ separating both levels is estimated to be 0.45 meV. By taking this observation into consideration, we suppose that the metastable level 1 consists of two sublevels locating close to each other. It is, therefore, suggested that the main band II originates from three excited triplet states separated by Δ and δ, where $\Delta >> \delta$. The lowest-lying level is thought to have a

small radiative transition probability, because its decay time is very long [29].

The excited states responsible for band I are somewhat peculiar, because it exhibits $P < 0$ or $P > 0$, depending on whether the excitation light is polarized with $\mathbf{E}_{ex}//\mathbf{c}$ or $\mathbf{E}_{ex}\perp\mathbf{c}$. To account for this observation, two requirements are imposed; (1) band I is ascribed to, at least, two excited states having an opposite polarization, and (2) the polarization memory of excitation light is preserved in the course of the nonradiative relaxation from optically created states to the emitting states. Realization of (2) is found, for instance, in resonant secondary emission from the F centers in alkali halides [30, 31], but it is not so much frequent as exceptional.

In ionic materials like metal halides and tungstates, depolarization is expected to take place efficiently during the nonradiative relaxation process through the strong coupling of electrons with lattice vibrations [32]. Even though optically created electrons lose their polarization memory, however, polarized luminescence is observable when the emitting state holds a proper polarization nature. This is really the case for bands II and III. On the other hand, the band I differs from the other two bands in two aspects. First, its peak energy is the highest among the three intrinsic bands, indicating that the relaxation energy into state I is relatively small. Second, its band width is remarkably narrow compared to those of bands II and III. This fact may imply a weak coupling of electrons in the state I with lattice vibrations. Unfortunately, the problem concerning the band I is of so complexity that we cannot suggest a plausible explanation for the reason why the requirement (2) is met for this band.

The band III gives a negative value of P as large as –0.14. This value is independent of the polarization of excitation light and also the temperature, indicating a simple nature of band III. It is therefore likely that this band will be attributed to a single triplet state emitting the luminescence polarized in the $\mathbf{E}\perp\mathbf{c}$ direction.

Summing up the results of the above discussions, we propose an energy-level diagram of the luminescent triplet states in PWO. That is illustrated in Fig. 9, in which the relationship between the sublevels in C_{3v} and C_s symmetry is also shown. Note that the order of the sublevels in C_{3v} is different between Figs. 1 and 9. From the optically detected EPR experiments of scheelite $CaMoO_4$ [16], it is important to note that the compressive crystal

field is considerably weak compared to the JT coupling, which means that the lowering of symmetry of $(WO_4)^{2-}$ ions upon excitation from C_{3v} to C_s is not so significant. If this is also the case for PWO, among $A'(\mathbf{x})$ and $A'(\mathbf{z})$ derived from A_1, the latter is more predominant than the former, and among $A'(\mathbf{x})$ and $A'(\mathbf{z})$ derived from E, the former becomes a major component. In Fig. 9, the minor components are enclosed in parentheses.

The level assignment is as follows:

(1) The state I consists of two sublevels $A'(\mathbf{x})$ [$P > 0$] and $A''(\mathbf{y})$ [$P < 0$]. When a PWO crystal is stimulated with $\mathbf{E}_{ex}//\mathbf{c}$ ($\mathbf{E}_{ex}\perp\mathbf{c}$) polarized light at 266 nm, the excited electrons preferentially relax into the $A''(\mathbf{y})$ level ($A'(\mathbf{x})$ level).

(2) The state II consists of three sublevels $A'(\mathbf{z})$ [$P < 0$], $A'(\mathbf{x})$ [$P > 0$] and $A''(\mathbf{y})$ [$P < 0$]. The negatively polarized levels $A'(\mathbf{z})$ and $A''(\mathbf{y})$ locate 72 meV above and 0.45 meV below the positively polarized level $A'(\mathbf{x})$, respectively. At moderate low temperatures ($T \approx 20$–100 K), thermal equilibrium between $A'(\mathbf{x})$ and $A''(\mathbf{y})$ is achieved, and the resulting luminescence could be polarized with $\mathbf{E}//\mathbf{c}$, because the radiative transition probability of level $A'(\mathbf{x})$ is much greater than that of level $A''(\mathbf{y})$. For very low temperatures, the existence of level $A''(\mathbf{y})$ is no longer negligible; i.e., the amount of P is expected to reduce to some extent. In Fig. 5, one may see a gradual decrease in P as a sample is cooled below 25 K. Such a decreasing tendency supports the existence of level $A''(\mathbf{y})$, although it is difficult to make a solid conclusion at present.

(3) The state III is likely assigned to the level $A''(\mathbf{y})$ [$P < 0$].

As pointed out in Introduction, it would be supposed that the relaxed excited states I, II and III correspond to three APES minima in the multidimensional configuration coordinate diagram proposed by Bacci *et al*. [14, 15].

Finally, we consider the polarization of the long-lived band IV appearing at 490 nm. As reviewed by Nikl [8], there is a broad consensus that this green luminescence arises from the radiative recombination of relaxed excitons perturbed by nearby lattice defects. The nature of the lattice defects has still been unclear, however. There may be two possible explanations for the polarization characteristic of band IV. One is applicable to the case that the perturbation by nearby defects is strong. In this case, the excited triplet states can be, to a

certain extent, deformed by them. If the electric dipole moment of such deformed triplet states is oriented parallel or perpendicular to the *c* axis, they could emit the luminescence polarized with **E**//**c** or **E**⊥**c**. The other is applicable to the case of the weak perturbation. In such a case, the excited triplet states of relaxed excitons are expected to be similar to those of STEs. The polarization of band IV is dependent on the temperature at least in the range $T >$ 150 K, as seen in Fig. 6. Since this dependence resembles the result of band II, defect-related IV state is thought to be a replica of the state II in pure PWO. Very recently, Babin *et al*. [33, 34] have claimed that two types of green emission bands, locating close to each other, exist in PWO, and they are of different origin. Therefore, the situation relating to the green luminescence might be more complicated than one expects. Further discussions on the state IV are beyond the scope of this paper.

5. Summary

In the present work, we have studied the polarization characteristics of time-resolved luminescence spectra of oriented PWO crystals in a wide temperature range T = 8–300 K. The results clearly reveal that the intrinsic bands I, II and III, as well as the extrinsic band IV, are significantly polarized in the *ac* plane. The main band II at 425 nm is polarized with **E**//**c** at low temperatures ($T <$ 100 K), but changes its polarization to **E**⊥**c** at $T >$ 150 K. The band III at 450 nm is polarized with **E**⊥**c** at T = 230 and 300 K. The band I at 407 nm exhibits $P <$ 0 or $P > 0$, depending on whether the excitation light is polarized with $\mathbf{E}_{\mathbf{ex}}$//**c** or $\mathbf{E}_{\mathrm{ex}}$⊥**c**. The symmetry lowering of tetrahedral $(WO_4)^{2-}$ ions due to the JT effect, which was suggested in our previous paper ([11]), is shown to be rather insufficient to account for the observed polarization characteristics of these bands. Further lowering of symmetry of $(WO_4)^{2-}$ due to the compressive crystal field is invoked. The sublevels of the lowest triplet STEs responsible for bands I, II and III are group-theoretically assigned on the basis of the C_s symmetry, with a realistic assumption that the crystal field is weaker than the JT coupling. We believe that the present study provides us with important information on the electronic structure of the luminescent triplet STEs in a representative scheelite-type tungstate, PWO.

One question, however, remains unanswered. That is why the A''(**y**) sublevel (A'(**x**)

sublevel) of the emitting state I is preferentially populated by optically created electrons under the excitation with 266 nm light polarized parallel (perpendicular) to the crystal *c* axis. Further study is required to answer this question. We are now involved in a similar study of the polarization of time-resolved luminescence spectra in $PbMoO_4$.

Acknowledgments

The authors would like to express their deepest gratitude to Prof. M. Fujita of Japan Coast Guard Academy for invaluable advices, particularly on the group-theoretical consideration of the lowest triplet sublevels of STEs in PWO. They are also grateful to Dr. Y. Usuki of the Materials Research Laboratory of Furukawa Co., Tsukuba, for providing the oriented single crystals used in the present experiments, and H. Mitani, S. Matsubayashi, K. Kasashima and T. Kajitani for kind help in preparation of the manuscript.

References

[1] R. W. G. Wyckoff, *Crystal Structures* (John Wily & Sons, New York, 1965) 2nd ed., Vol. 3, Chapter VIII.

[2] P. F. Schofield, K. S. Knight, S. A. T. Redfern and G. Cressey, Acta Crystallogr., Sect. B, **53**, 102 (1997).

[3] M. Kobayashi, M. Ishii, Y. Usuki and H. Yahagi, Nucl. Instrum. Methods Phys. Res. A, **333**, 429 (1993).

[4] P. Lecoq, I. Dafinei, E. Auffray, M. Schneegans, M. V. Korzhik, O. V. Missevitch, V. B. Pavlenko, A. A. Fedorov, A. N. Annenkov, V. L. Kostylev and V. D. Ligun, Nucl. Instrum. Methods Phys. Res. A, **365**, 291 (1995).

[5] W. W. Moses, in *Proceedings of the Fifth International Conference on Inorganic Scintillators and Their Applications*, edited by V. Mikhailin (Moscow State University, Moscow, 2000), p. 11.

[6] M. Kobayashi, Y. Usuki, M. Ishii, M. Itoh and M. Nikl, Nucl. Instrum. Methods Phys. Res. A, **540**, 381 (2005).

[7] J. A. Groenink and G. Blasse, J. Solid State Chem., **32**, 9 (1980).

[8] M. Nikl, Phys. Status Solidi A, **178**, 595 (2000).

[9] G. Blasse, Struct. Bonding, **42**, 1 (1980).

[10] M. Itoh and T. Sakurai, Phys. Status Solidi B, **242**, R52 (2005).

[11] M. Itoh and T. Sakurai, Phys. Rev. B, **73**, 235106 (2006).

[12] A. Fukuda, Phys. Rev. B, **1**, 4161 (1970).

[13] M. Bacci, A. Ranfagni, M. P. Fontana and G. Viliani, Phys. Rev. B, **11**, 3052 (1975).

[14] M. Bacci, S. Porcinai, E. Mihóková, M. Nikl and K. Polák, Phys. Rev. B, **64**, 104302 (2001).

[15] M. Bacci, E. Mihóková and L. S. Schulman, Phys. Rev. B, **66**, 132301 (2002).

[16] W. Barendswaard and J. H. van der Waals, Molec. Phys., **59**, 337 (1986).

[17] J. van Tol, J. A. van Hulst and J. H. van der Waals, Molec. Phys., **76**, 547 (1992).

[18] J. van Tol and J. H. van der Waals, Molec. Phys., **88**, 803 (1996).

[19] W. van Loo, Phys. Status Solidi A, **28**, 227 (1975).

[20] M. V. Korzhik, V. B. Pavlenko, T. N. Timoschenko, V. A. Katchanov, A. V. Singovskii, A. N. Annenkov, V. A. Ligun, I. M. Solskii and J. -P. Peigneux, Phys. Status Solidi A, **154**, 779 (1996).

[21] E. G. Reut, Izv. Akad. Nauk SSSR, **43**, 1186 (1979).

[22] E G. Reut, Opt. Spectrosc., **57**, 90 (1984).

[23] M. Fujita, M. Itoh, M. Horimoto and H. Yokota, Phys. Rev. B, **65**, 195105 (2002).

[24] C. Itoh and S. Kigoshi, Phys. Status Solidi A, **203**, 3774 (2006).

[25] M. Itoh, M. Horimoto and M. Fujita, J. Phys.: Condens. Matter, **15**, 193 (2003).

[26] E. Gürmen, E. Daniels and J. S. King, J. Chem. Phys., **55**, 1093 (1971).

[27] V. Mürk, M. Nikl, E. Mihoková and K. Nitsch, J. Phys.: Condens. Matter, **9**, 249 (1997).

[28] Z. Han, C. Shi, G. Zhang, J. Shi, G. Zimmerer and B. Steeg, J. Electron Spectrosc. Relat. Phenom., **101-103**, 583 (1999).

[29] M. Nikl, P. Bohacek, E. Mihokova, M. Kobayashi, M. Ishii, Y. Usuki, V. Babin, A. Stolovich, S. Zazubovich and M. Bacci, J. Lumin., **87-89**, 1136 (2000).

[30] Y. Mori, R. Hattori and H. Ohkura, J. Phys. Soc. Jpn., **51**, 2713 (1982).

[31] N. Akiyama, S. Muramatsu and A. Tsuchihashi, J. Phys. Soc. Jpn., **70**, 1417 (2001).

[32] Y. Toyozawa, *Optical Processes in Solids* (Cambridge University Press, Cambridge, 2003), Chapter 4.

[33] V. Babin, P. Bohacek, E. Bender, A. Krasnikov, E. Mihokova, M. Nikl, N. Senguttuvan, A. Stolovits, Y. Usuki and S. Zazubovich, Radiat. Meas., **38**, 533 (2004).

[34] V. Babin, P. Bohacek, A. Krasnikov, M. Nikl, A. Stolovits and S. Zazubovich, J. Lumin., **124**, 113 (2007).

Figure captions

Figure 1. Schematic level diagram of the STEs in PWO suggested in [11]. The lowest triplet $^3T_2$ and $^3T_1$ states split into the $^3A_1$ and ^3E sublevels and the $^3A_2$ and ^3E sublevels, respectively, owing to the symmetry lowering from T_d to C_{3v}. It is not possible to determine whether the order of the triplet levels is as shown, or the reverse, from a group-theoretical consideration.

Figure 2. Time-resolved luminescence spectra measured for polarizations **E**//**c** (blue solid line) and **E**⊥**c** (blue broken line) at T = 75 K. The excitation was made by 266 nm light polarized parallel to the c axis (a) and perpendicular to it (b). The spectra in (a) and (b) are normalized to unity at their maxima measured for **E**//**c**, respectively.

Figure 3. Time-resolved luminescence spectra for (a) **E**//**c** and (b) **E**⊥**c** under the excitation by light polarized with $\mathbf{E}_{ex}$//**c** at T = 300 K. The spectra measured at the same delay time in (a) and (b) are normalized to unity at their maxima. The bands I, II, III and IV are depicted by violet dotted, blue solid, light-blue broken and green solid lines, respectively. The sum of these four bands is indicated by red solid line, in good agreement with the observed spectrum.

Figure 4. The same as in Fig. 3 but excited by light polarized with $\mathbf{E}_{ex}$⊥**c**.

Figure 5. Temperature dependence of the degree of polarization of band II. Black open circles refer to the results measured under the $\mathbf{E}_{ex}$//**c** excitation, and red closed circles to those under the $\mathbf{E}_{ex}$⊥**c** excitation. The solid line is the best-fitted curve of Eq. (4) to the experimental points. The inset illustrates a two-level model to account for the thermal change of P, the details of which are described in the text.

Figure. 6. Temperature dependences of the degree of polarization of bands I (circles), III

(triangles) and IV (squares). Open symbols refer to the results measured under the $\mathbf{E}_{ex}$//**c** excitation, and closed symbols to those under the $\mathbf{E}_{ex}\perp$**c** excitation. The solid lines are depicted only for guide to the eye.

Figure. 7. (a) A tetrahedral $(WO_4)^{2-}$ ion with respect to the crystal *c* axis. One tungsten (W) and four oxygen (O_1, O_2, O_3 and O_4) ions are depicted by open and gray circles, respectively. (b) A JT-distorted $(WO_4)^{2-}$ ion with C_{3v} symmetry. The *z* axis lies exactly along the W–O_1 bond and coincides with the triad axis. The *x* and *y* axes are perpendicular to the *z* axis. There are four equivalent JT-distorted $(WO_4)^{2-}$ ions that are found by $\pi/2$ rotation about the *c* axis.

Figure 8. An excited $(WO_4)^{2-}$ ion with C_s symmetry. One tungsten (W) and four oxygen (O_1, O_2, O_3 and O_4) ions are depicted by open and red circles in relation to the crystallographic axes, respectively. The four oxygen ions in the ground state are also shown by gray circles for reference. The mirror plane σ_d spanned by O_1–W–O_2 is the only symmetry element in C_s symmetry. The *y* fine-structure axis is almost perpendicular to the σ_d plane. The *z* fine-structure axis is close to the direction of W–O_1 bond and lies together with the *x* fine-structure axis approximately in the σ_d plane.

Figure 9. A proposed level diagram of the triplet STEs in PWO in an arbitrary energy scale. Because of the symmetry lowering from C_{3v} to C_s, the state *E* splits into the sublevels $A'(\mathbf{x})$ (or $A'(\mathbf{z})$) and $A''(\mathbf{y})$, and the states A_1 and A_2 transform to the sublevels $A'(\mathbf{z})$ (or $A'(\mathbf{x})$) and $A''(\mathbf{y})$, respectively. The $A'(\mathbf{z})$ derived from *E* and the $A'(\mathbf{x})$ derived from A_1 are both a minor component (indicated in parentheses), when the crystal field is not so strong compared to the JT coupling. The order of the sublevels in C_{3v} is changed with respect to that in Fig. 1.

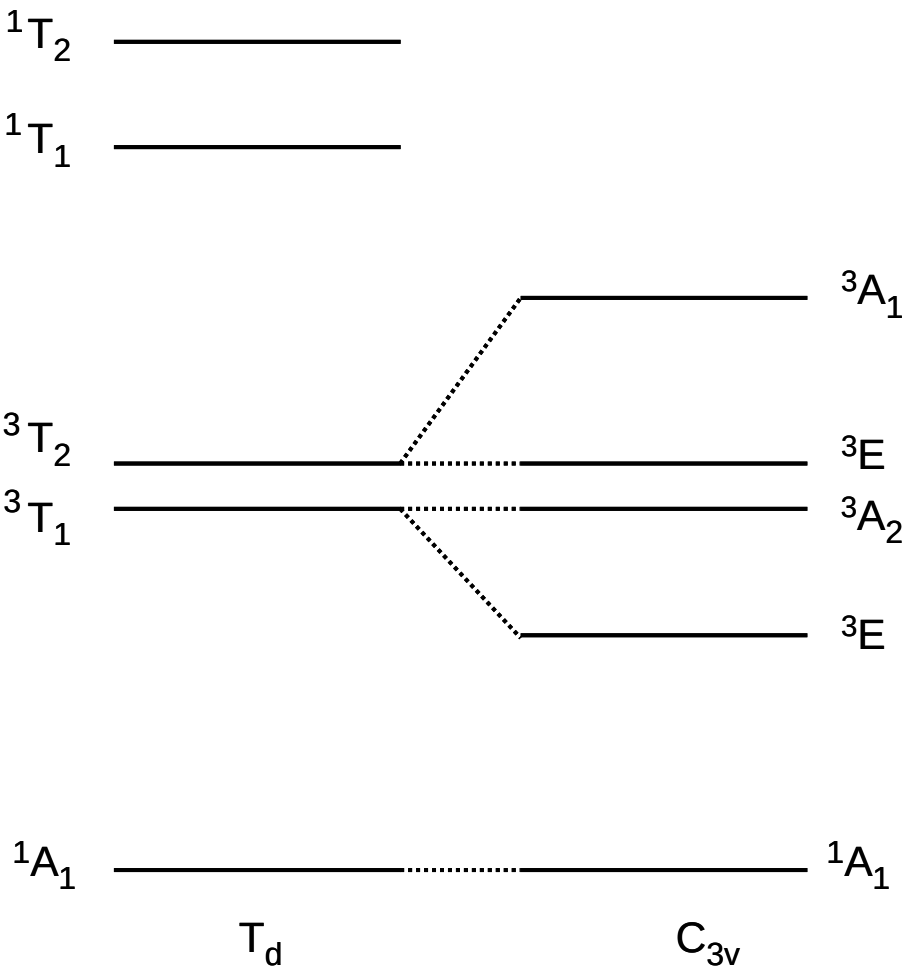

Fig. 1

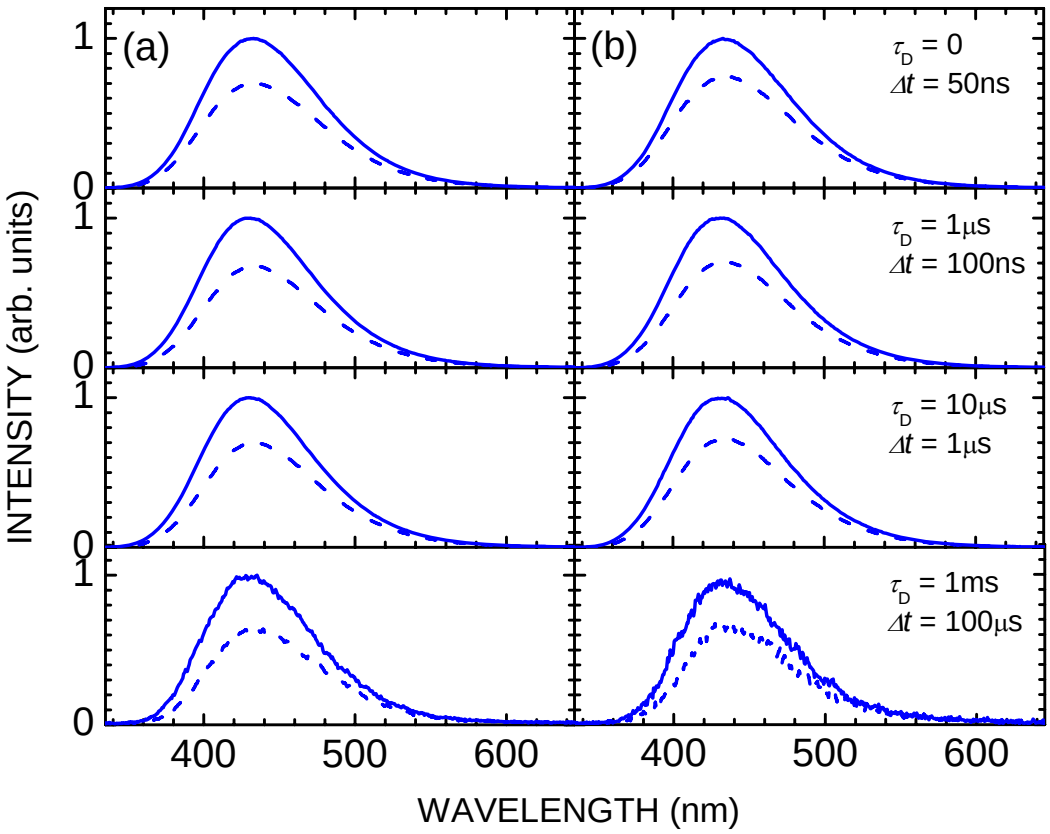
(a)
(b)
τ_D = 0
Δt = 50ns
τ_D = 1μs
Δt = 100ns
τ_D = 10μs
Δt = 1μs
τ_D = 1ms
Δt = 100μs
INTENSITY (arb. units)
WAVELENGTH (nm)
0
1
400
500
600

Fig. 2

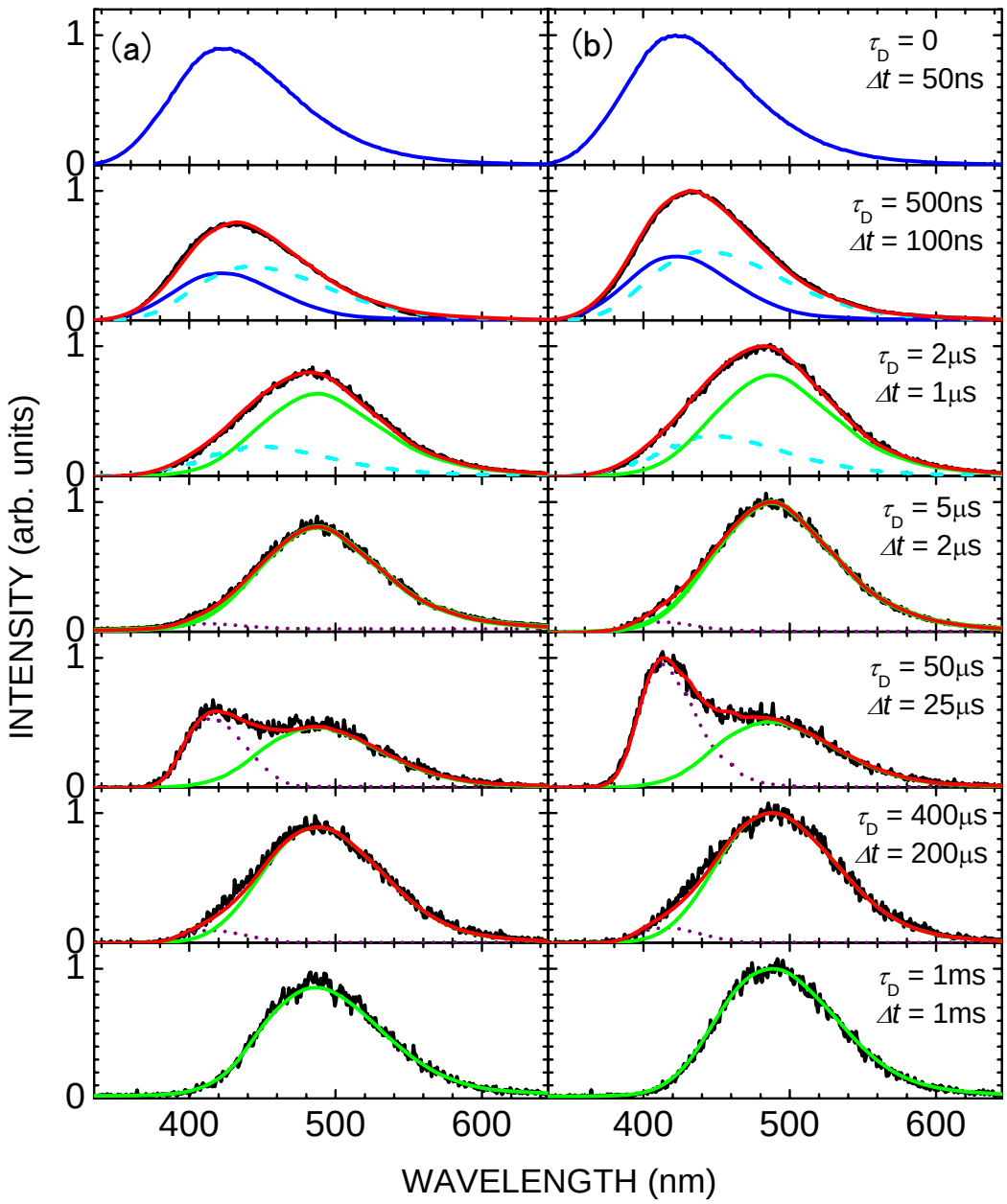
(a)
(b)
τ_D = 0
Δt = 50ns
τ_D = 500ns
Δt = 100ns
τ_D = 2μs
Δt = 1μs
τ_D = 5μs
Δt = 2μs
τ_D = 50μs
Δt = 25μs
τ_D = 400μs
Δt = 200μs
τ_D = 1ms
Δt = 1ms
INTENSITY (arb. units)
WAVELENGTH (nm)
0
1
400
500
600

Fig. 3

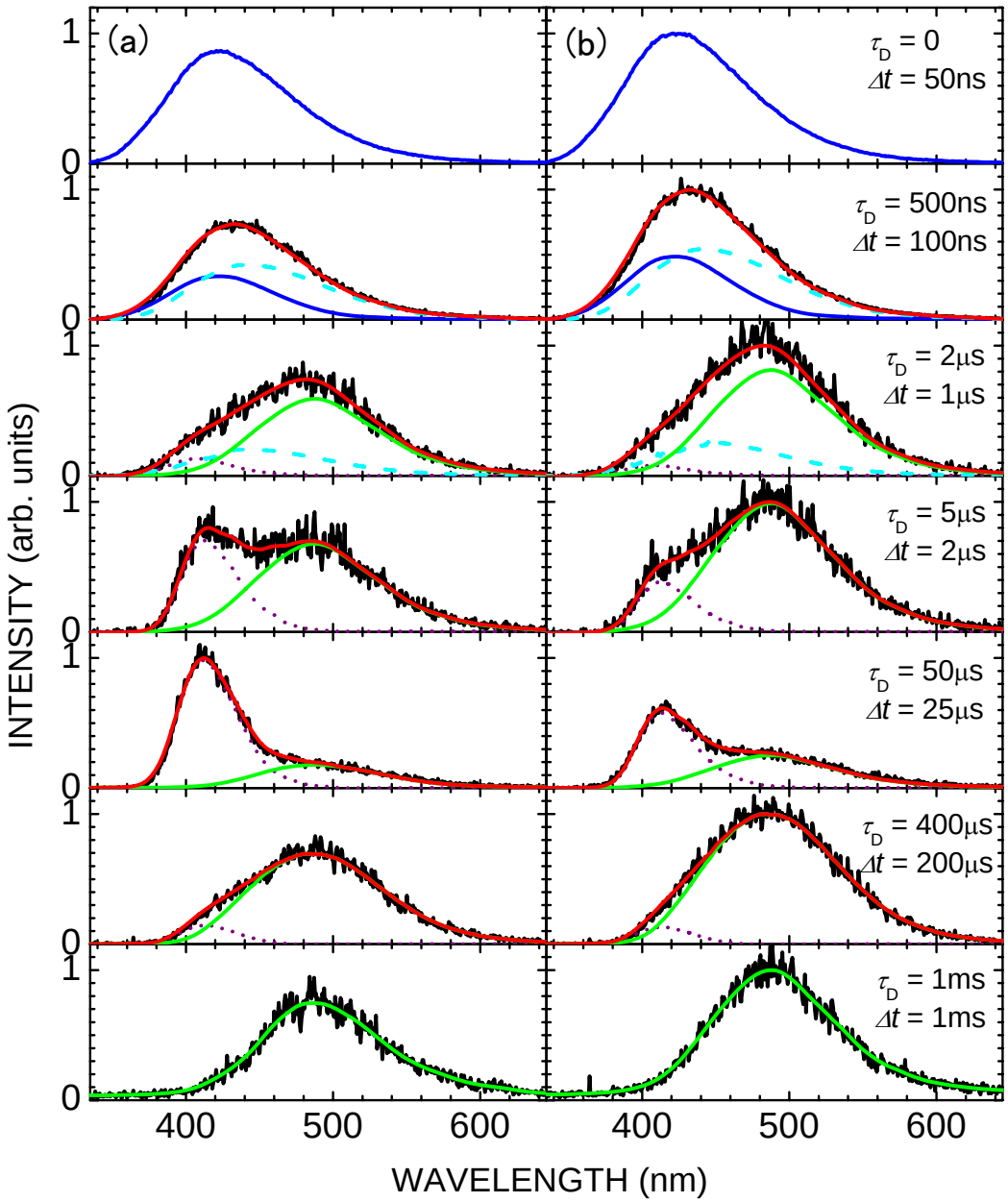
(a)
(b)
τ_D = 0
Δt = 50ns
τ_D = 500ns
Δt = 100ns
τ_D = 2μs
Δt = 1μs
τ_D = 5μs
Δt = 2μs
τ_D = 50μs
Δt = 25μs
τ_D = 400μs
Δt = 200μs
τ_D = 1ms
Δt = 1ms
INTENSITY (arb. units)
WAVELENGTH (nm)
0
1
400
500
600

Fig. 4

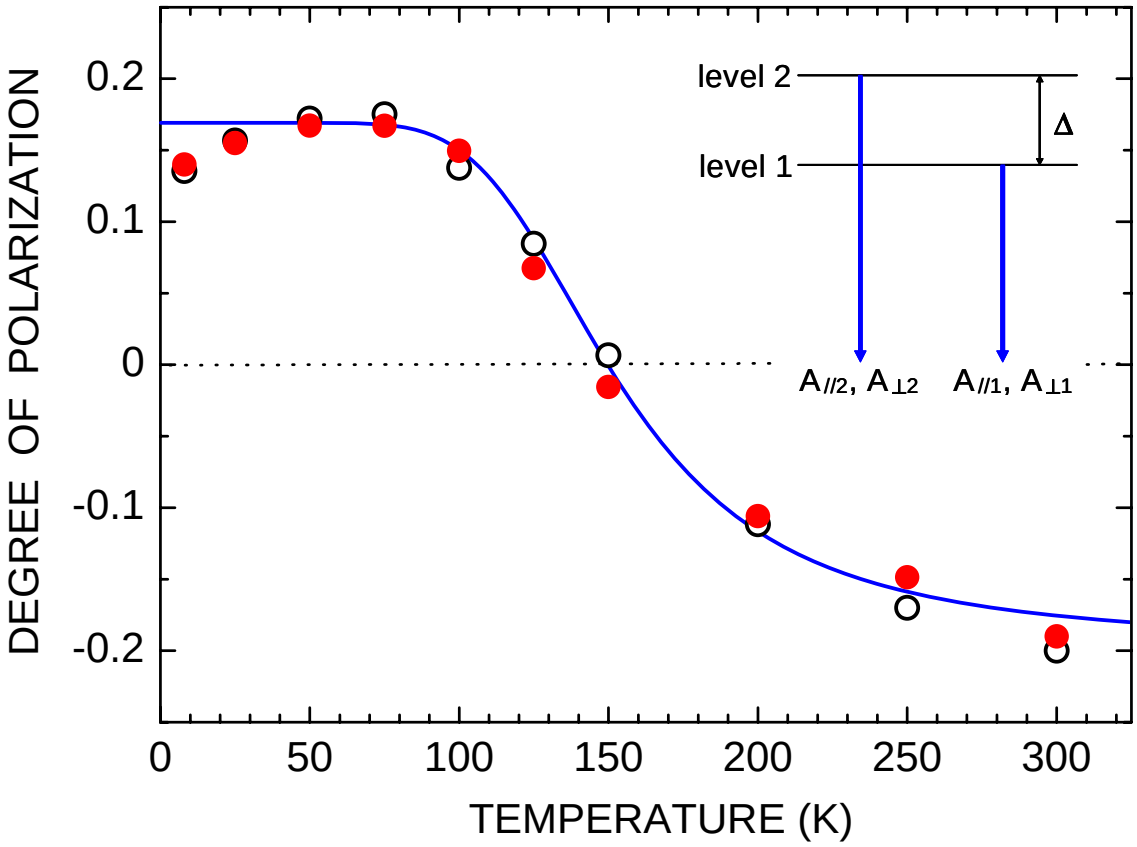
DEGREE OF POLARIZATION
0.2
0.1
0
-0.1
-0.2
0
50
100
150
200
250
300
TEMPERATURE (K)
level 2
level 1
Δ
A//2, A⊥2
A//1, A⊥1

Fig. 5

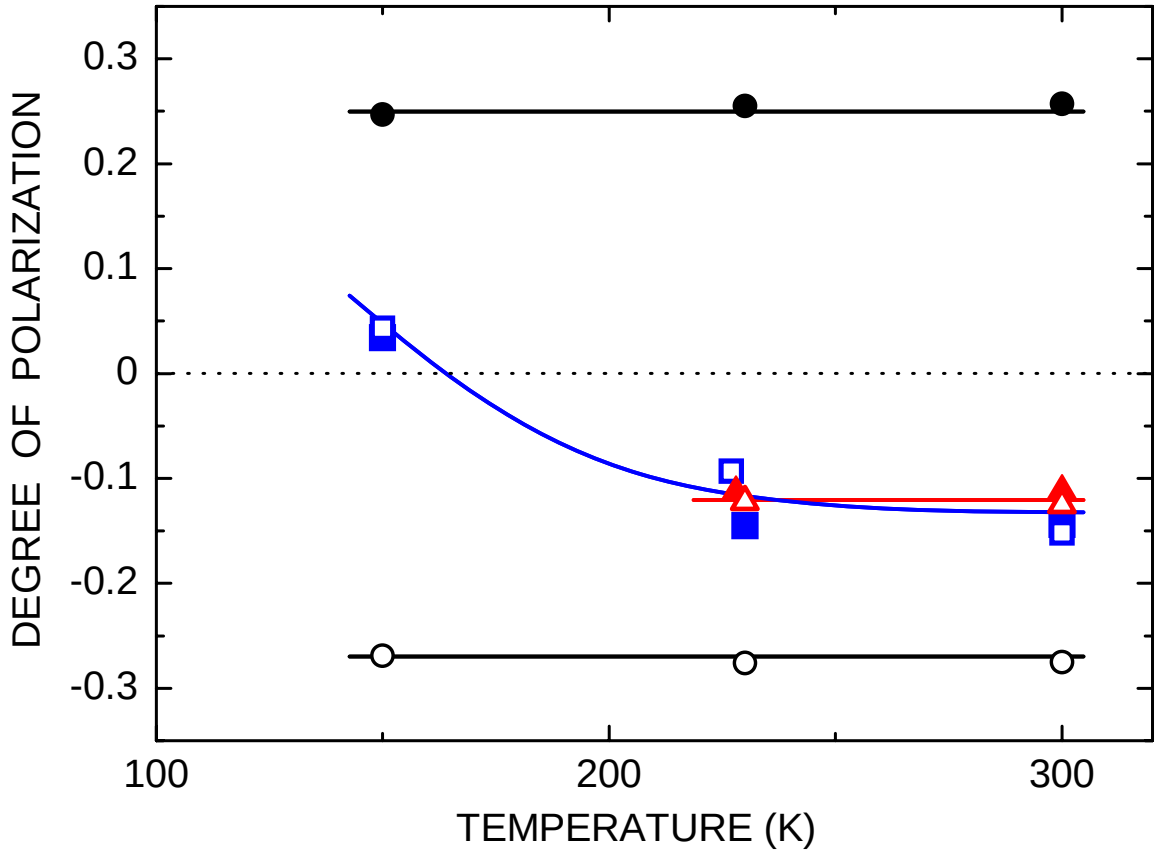
DEGREE OF POLARIZATION
0.3
0.2
0.1
0
-0.1
-0.2
-0.3
100
200
300
TEMPERATURE (K)

Fig. 6

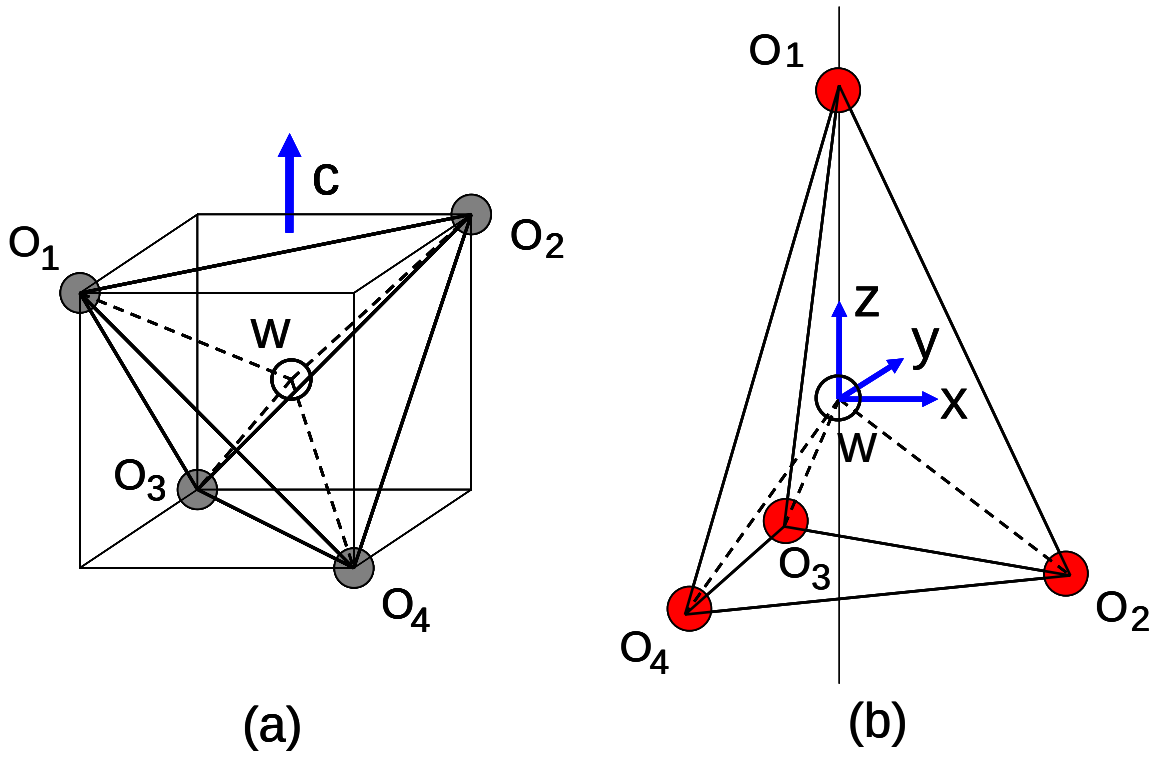

Fig. 7

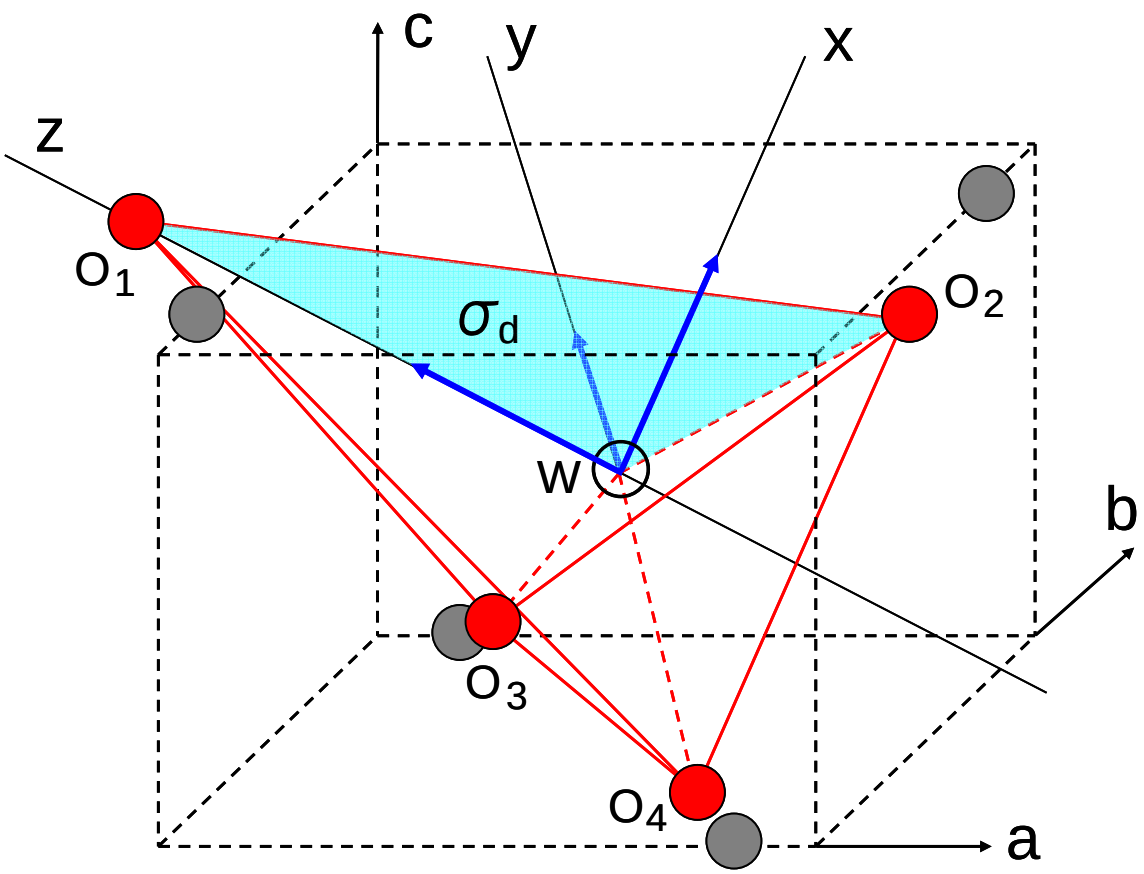

Fig. 8

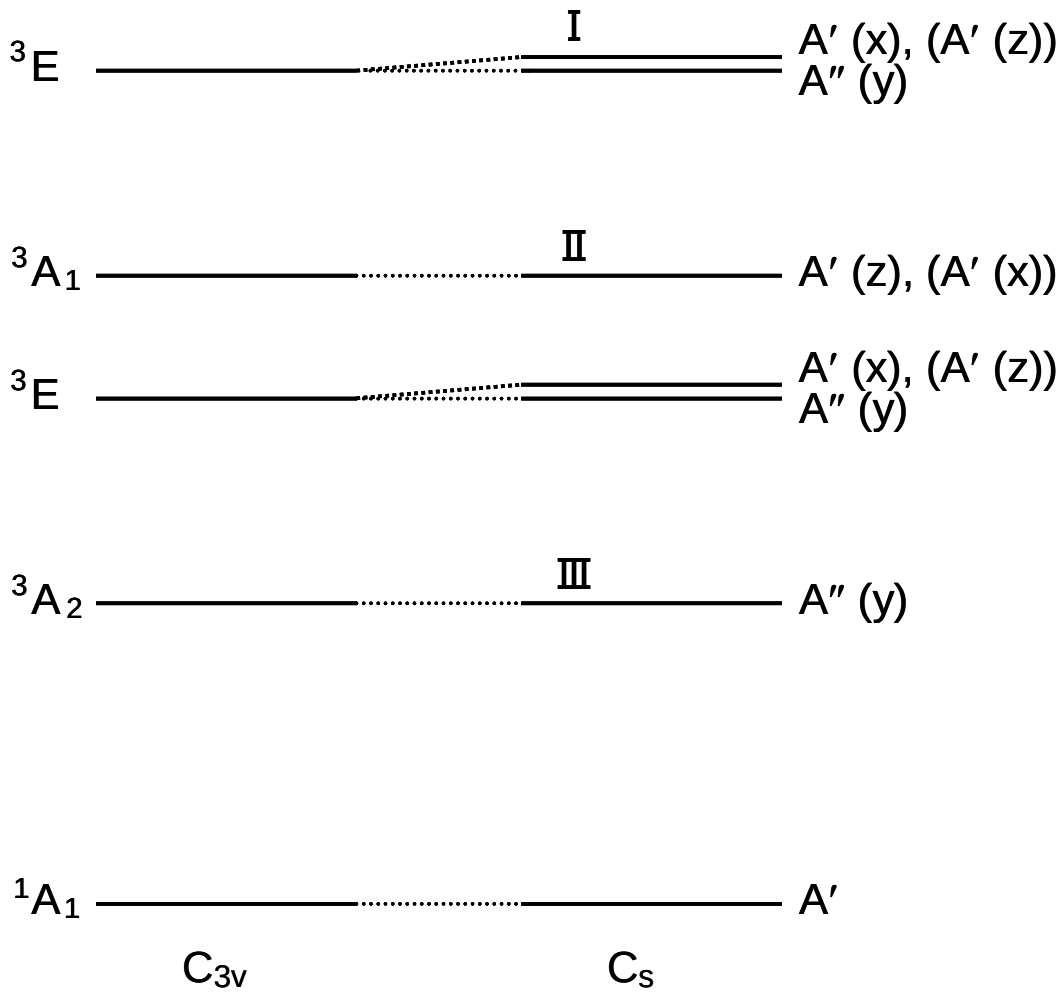

Fig. 9